Sichao Su ✉
Ruiqing Li
Yi Zhou

https://doi.org/10.21278/TOF.484061523
ISSN 1333-1124
eISSN 1849-1391

THE EFFECT OF ULTRASOUND ON THE LONGITUDINAL SECTION OF A 2A14 ALUMINIUM ALLOY INGOT WITH A DIAMETER OF 830 MM

Summary

In the casting experiment of a 2A14 aluminium alloy ingot with a diameter of 830 mm, a comparison was made between the method when ultrasonic treatment was applied and the method when ultrasonic treatment was not applied. In the ingot which was not subjected to the ultrasonic treatment, the segregation rates of Cu and Si elements on a 1/2 longitudinal section were 29.98% and 27.96%, respectively. The average tensile strength, average yield strength and average elongation were 169.50 MPa, 87.17 MPa, and 5.32%, respectively. In the case of the ultrasonically treated ingot, the segregation rates of Cu and Si elements were 28.15% and 21.51%, respectively, and the average tensile strength, average yield strength and average elongation were 178.38 MPa, 92.75 MPa and 7.10%, respectively. The average tensile strength, average yield strength and average elongation of the ultrasonically treated ingot were increased by 5.24%, 6.40% and 33.46%, respectively. The results showed that after the ultrasonic treatment, the macro-segregation was inhibited, the defects were reduced, and the eutectic structure was more uniform.

Key words: *ultrasonic treatment, macro-segregation, eutectic structure*

1. Introduction

As important light metallic materials, aluminium alloys are widely used in many fields. Large aluminium alloy ingots are often produced using the direct casting process. In this process, it is easy to cause macro-segregation in the ingot [1, 2]. Therefore, in order to reduce segregation in ingots, green, non-polluting ultrasound is often used in casting. Ultrasonic treatment of aluminium melts can produce acoustic flow, cavitation, and other effects [3, 4]. Eskin D. G. considered the theoretical and application aspects of the ultrasonic melt treatment [3]. The industrial applications of the ultrasonic cavitation effect in degassing, filtration, and grain refinement are illustrated with the data of commercial alloys. Eskin D. G. reviewed the mechanisms involved in the ultrasonic melt treatment, including cavitation, flow, nucleation, activation, fragmentation, and their effects on degassing, structural refinement, and particle dispersion [4] .

Segregation phenomenon occurs in aluminium alloy ingots with different diameters and grades treated by direct casting technology. Li et al. found that a grain-refined structure with

reduced macro-segregation was obtained in the large-scale cylindrical Al alloy ingot (650 mm in diameter, 4,800 mm in length) [5] . Li et al. used special DC casting equipment to manufacture a large cylindrical AA2219 aluminium alloy ingot (1,250 mm in diameter and 3,300 mm in length) [6] . The macro-segregation of the main element (Cu) at different casting stages was measured on three cross sections of an as-cast ingot. By establishing a theoretical model, Fezi K. found that the depth of the molten pool, the steady-state height, and the macro-segregation level were most affected by changes in the casting speed and the ingot diameter [7]. Through an analysis of 15 t of AA2219 aluminium alloy ingots Zeng T. found that the application of ultrasound during solidification can reduce interdendritic micro-segregation of equiaxed grains, can inhibit macro-segregation of chemical components in the ingot, and obtain a more uniform micro-structure [8]. Peng H. studied the effect of ultrasound on the micro-structure and macro-segregation of ingots by changing the position and power parameters of ultrasound [9]. The combined effects of ultrasound on flow, heat transfer, and grain movement weaken the segregation of Cu. Li A. compared the effects of double-source ultrasound and three-source ultrasound on ingots (630 mm in diameter and 4,500 mm in length) and found that the degassing efficiency of three-source ultrasound was higher than that of double-source ultrasound, with a more uniform distribution of Cu elements [10]. Wang K. studied the casting of large Al-Cu ingots (830 mm in diameter and 6,000 mm in length) under different ultrasonic processing conditions (using a single ultrasonic electrode and four ultrasonic electrodes) [11]. After the ultrasonic melting treatment α-Al grains were refined again. At the same time, the macro-segregation of Cu in the ingot was improved, and the area fraction of the coarse Al_2Cu eutectic phase was reduced. Zhang L. studied an ultra-large AA2219 Al alloy ingot (1.38 m in diameter and 4.6 m in length) which was manufactured using a direct chill casting technique assisted by four ultrasonic sonotrodes [12]. Zhang Li found that the macro-segregation of the main element (Cu) was alleviated.

Shi C. studied the effect of ultrasonic vibration on the solidification structure and component segregation of large ingots during the semi-continuous casting of a 2A14 aluminium alloy [13]. The results showed that during the solidification process of the 2A14 aluminium alloy, ultrasonic treatment could reduce the macro-segregation of a solute, including negative segregation at the edge of the ingot and positive segregation at the centre. At present, there is not much literature on the large-scale ultrasonic assisted casting of 2A14 aluminium alloys. (2A14 aluminium alloy is a Chinese grade, and the American grade for this aluminium alloy is 2014.)

In addition, most of the studies mainly focused on the cross section of the ingots, but few focused on the longitudinal section of ingots. This paper will focus on the longitudinal section of a 2A14 aluminium alloy ingot.

2. Experimental equipment and process

2.1 Semi-continuous casting equipment

The main purpose of the experiment was to obtain a 2A14 aluminium alloy ingot with a diameter of 830 mm and length of 5,500 mm. The main equipment includes: a 20 t smelting furnace and semi-continuous casting system, a chute degassing device, a filtering device, a crystallizer, an ultrasonic vibration system and other auxiliary equipment. The image of ultrasonic assisted casting is shown in Fig. 1(a). The numbers 1 to 9 in Fig. 1(b) represent the casting channel, hot top, ultrasonic generator, sonotrode, aluminium melt, crystallizer, cooling water outlet, solidified area and ingot guiding device, respectively.

2.2 Semi-continuous casting procedure

Before the experiment, it was necessary to debug the whole experimental equipment to ensure that each link could operate correctly. According to the composition ratio of the 2A14

aluminium alloy and considering the chemical activity of the alloying elements, one way was to prepare pure aluminium and binary aluminium alloy in proportion, and the other way was to prepare pure aluminium and required alloying elements in proportion. In this study, these two methods were combined, and the material was placed in a resistance furnace. After the aluminium alloy material was completely melted, electromagnetic stirring and slag raking treatment were carried out to ensure the purity of the molten liquid.

After the molten liquid composition met the requirements, the casting channel and crystallizer were cleaned and preheated. When the casting conditions had been met, the control system opened the furnace mouth, and the molten aluminium flowed into the crystallizer along the casting channel, and the cooling water system was opened. After the molten aluminium filled the crystallizer, due to the low temperature of the crystallizer, the molten aluminium just flowing into the crystallizer cooled quickly and a molten pool formed in the crystallizer. After the molten pool had stabilized, the traction system was activated for semi-continuous casting.

In this study, a comparative experiment was conducted between the method in which ultrasound treatment was applied and the method in which ultrasound treatment was not applied. The ultrasound-assisted casting system consisted of an ultrasonic generator, a power supply, a waveguide, a vortex tube cooler, and a titanium sonotrode with a tip diameter of 50 mm. The sonotrode was preheated to minimise its cooling effect, before having been immersed in the alloy melt (200 mm below the top surface of the melt). The frequency of the ultrasonic generator was 20±1 kHz, and the peak-to-peak amplitude was 20±0.1 μm (The amplitude of the end face of the sonotrode was obtained by a laser rangefinder). After the sonotrode was inserted into the aluminium melt, the parameters of the generator were adjusted to ensure that the sonotrode vibration reached a steady state. The aluminium alloy casting experiment subjected to the ultrasonic treatment is shown in Fig. 1(a) and Fig. 1(b).

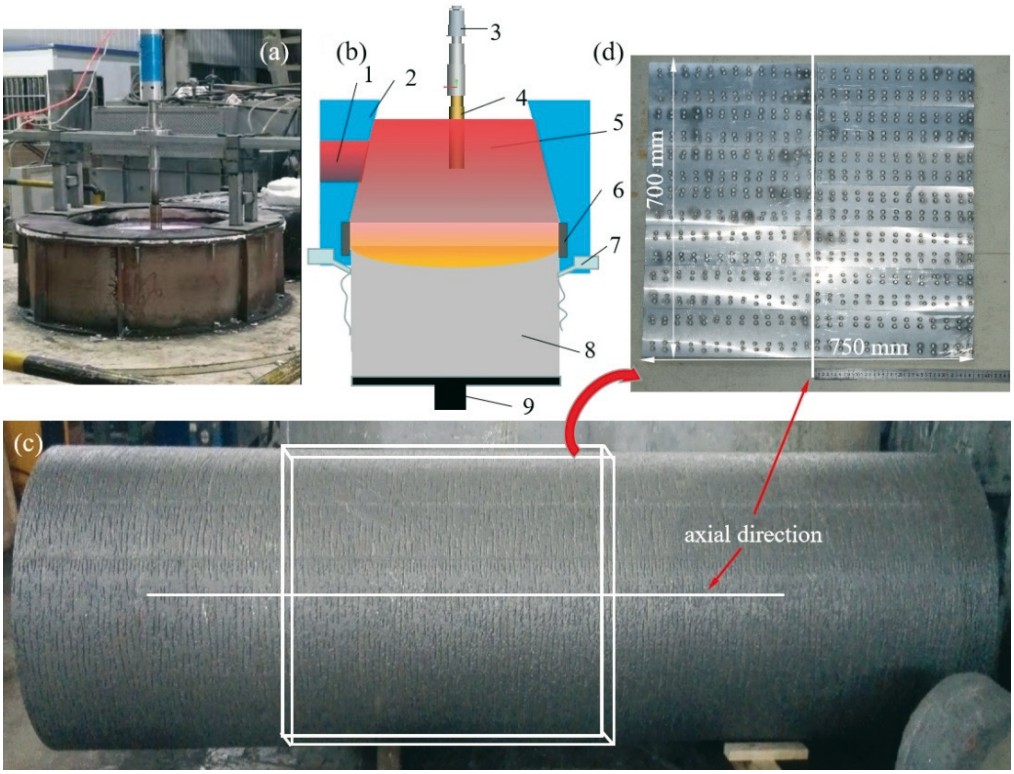

Fig. 1 Aluminium alloy casting: (a) ultrasonic casting of aluminium alloy, (b) casting schematic diagram, (c) ingot, (d) longitudinal section

A 2A14 aluminium alloy ingot with a diameter of 830 mm was obtained through the casting experiment, as shown in Fig.1(c). After cutting off the skin of the round ingot, the actual diameter of the ingot was 750 mm. An aluminium block with a length of 700 mm and a thickness of 20 mm was cut along the axis of the aluminium alloy ingot. The radial dimension of the aluminium block was still 750 mm. Then, the surface of the aluminium block was milled on a milling machine to make the surface smooth enough. The aluminium block obtained from the longitudinal section was cut into small pieces for component determination on a direct reading spectrometer, as shown in Fig. 1(d). The alloy composition of 2A14 aluminium alloy is shown in Table 1, with the highest content of Cu, followed by Si. Consequently, this paper mainly discusses the degree of segregation of these two elements.

Table 1 Composition of 2A14 aluminium alloy (%) [14]

Composition	Cu	Mg	Si	Mn	Ni	Zn	Fe	Ti	Al
Experimental material	4.37	0.63	0.93	0.78	<0.001	<0.001	0.1	0.026	Bal.
Reference	3.9-4.8	0.4-0.8	0.6-1.2	0.4-1.0	≤0.1	≤0.3	≤0.7	≤0.16	Bal.

3. Results and discussions

3.1 Distribution of Cu and Si in 2A14 aluminium alloy ingots with a diameter of 830 mm

By measuring the longitudinal section of the ingot, the contents of different elements were obtained, and the contents of the main solute elements Cu and Si were drawn into a cloud map. Fig. 2(a) and (c) show the distribution of the Cu and Si content of the ingot not subjected to the ultrasonic treatment, while Fig. 2(b) and (d) show the distribution of the Cu and Si content of the ingot subjected to the ultrasonic treatment, respectively.

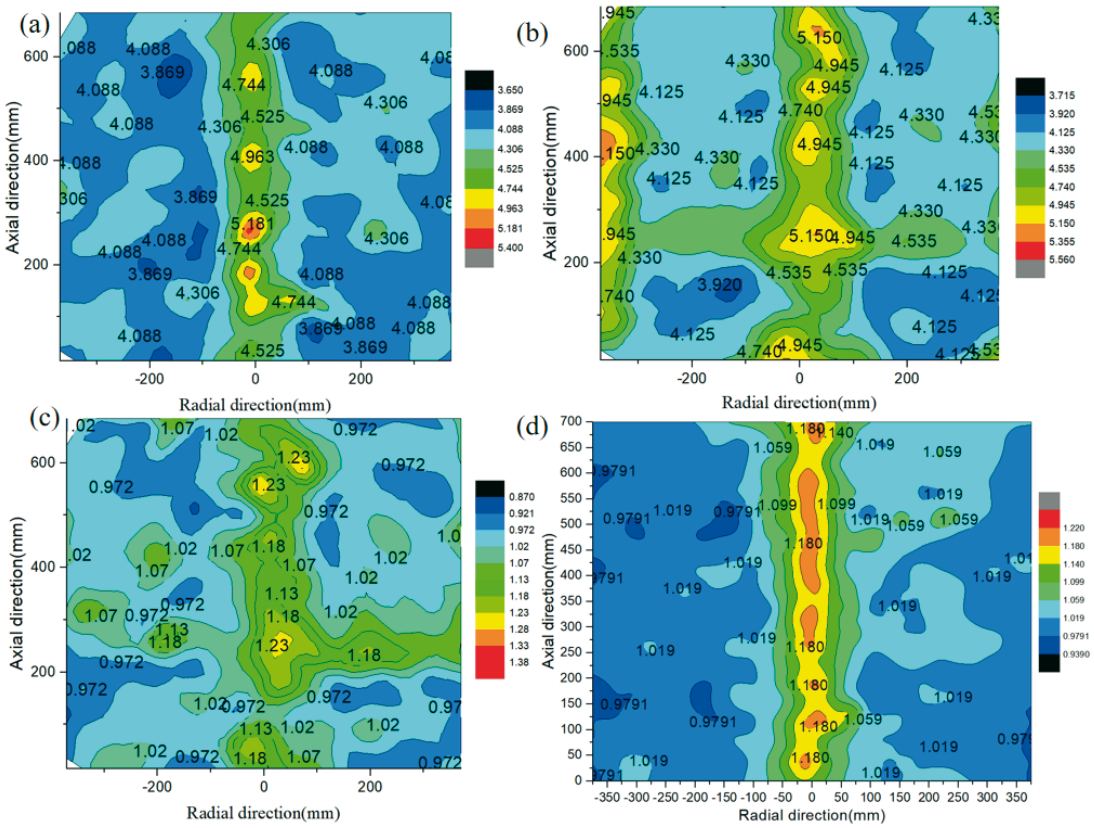

Fig. 2 Distribution map of main components: (a), (c) Cu and Si elements on longitudinal sections of the ingot not subjected to ultrasonic treatment; (b), (d) Cu and Si elements on longitudinal sections of the ingot subjected to ultrasonic treatment. (The numerical unit in the cloud map is %)

Segregation rate is an index which characterises the degree of segregation of the Cu and Si solutes. The formula of the segregation rate is as follows [15, 16]:

$$k = (C_{\max} - C_{\min}) / C_0 \tag{1}$$

where k is the segregation rate, C_{max} is the maximum concentration, C_{min} is the minimum concentration, and C_0 is the average concentration.

It can be seen from Fig. 2(a) that the maximum Cu content of the ingot not subjected to the ultrasonic treatment was 5.18%, and the minimum Cu content was 3.87%. It can be seen from Fig. 2(b) that the maximum and minimum Cu contents of the ingot subjected to the ultrasonic treatment were 5.15% and 3.92%, respectively. It can be seen from Fig. 2(c) that the maximum Si content of the ingot not subjected to the ultrasonic treatment was 1.23%, and the minimum Si content was 0.97%. It can be seen from Fig. 2(d) that the maximum and minimum Cu contents of the ingot subjected to the ultrasonic treatment were 1.18% and 0.98%, respectively. The segregation rates of the Cu and Si elements in the ingot not subjected to the ultrasonic treatment were 29.98% and 27.96%, respectively. For the ingot subjected to the ultrasonic treatment, the segregation rates of Cu and Si were 28.15% and 21.51%, respectively. Total amounts of the Cu and Si elements in the longitudinal section subjected to the ultrasonic treatment were more balanced.

3.2 Analysis of mechanical properties of the longitudinal section

The positions of the samples taken on the 1/2 longitudinal section of the ingot are shown in Fig. 3. Three tensile samples and one sample with a length, width, and height of 15 mm, 15 mm, and 20 mm were taken from each position shown in Fig. 3(a). Fig. 3(b) shows the specific location of the sampling, and Fig. 3(c) shows the specific dimensions of the tensile samples.

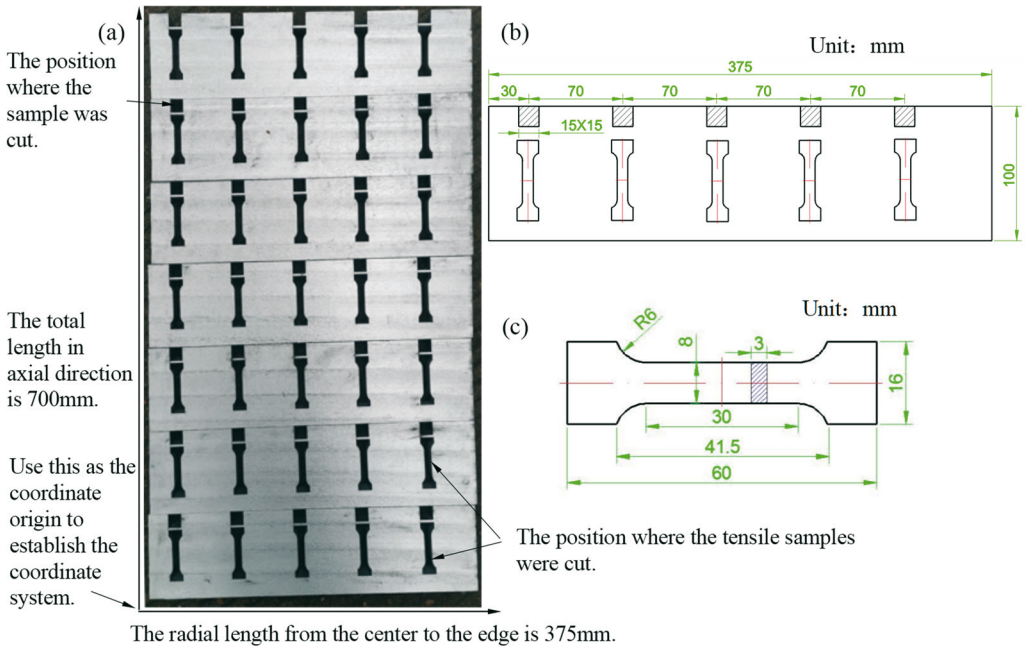

Fig. 3 Sampling diagram: (a) sampling on longitudinal section, (b) sampling position, (c) size of stretched sample

Fig. 3(a) shows a half longitudinal section of the ingot, where the lower left corner is used as the coordinate origin to establish a coordinate system. The samples taken at a distance of 30 mm from the centre of the ingot were the first column samples, and the samples taken at a

distance of 100 mm, 170 mm, 240 mm, and 310 mm from the centre were the second, third, fourth, and fifth column samples, respectively.

The average tensile strength of the first column samples that were not subjected to the ultrasonic treatment was 157.93 MPa, while the average tensile strength of the first column samples subjected to the ultrasound treatment was 167.81 MPa, which was 9.88 MPa higher than in the case when no ultrasonic treatment was applied. The average tensile strength improvement rate of the first column samples subjected to the ultrasonic treatment compared to the first column samples not subjected to the ultrasonic treatment was 6.25%. The average tensile strength of the second, third, fourth, and fifth column samples subjected to the ultrasonic treatment increased by 6.91%, 6.41%, 3.9%, and 3.25%, respectively, compared to the samples not subjected to the ultrasonic treatment. The maximum increase in the average tensile strength of the second column samples subjected to the ultrasonic treatment compared to those not subjected to the ultrasonic treatment was 6.91%. The improvement rate of the average tensile strength decreased with an increase in the distance from the centre, and the farther the distance, the weaker the ultrasonic effect.

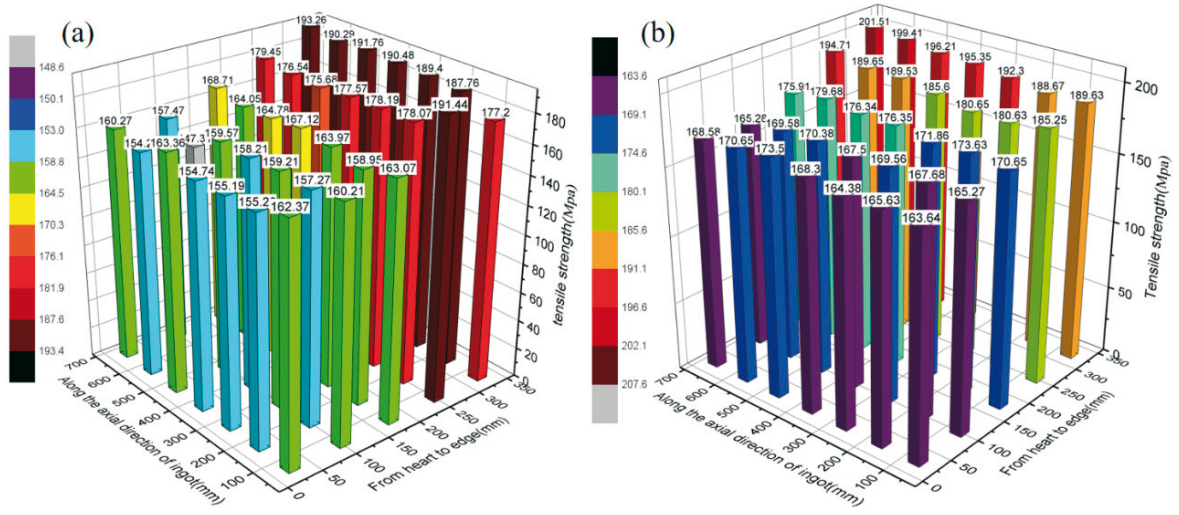

Fig. 4 Tensile strength distribution of 1/2 longitudinal section of ingot: (a) ultrasonic treatment not applied, (b) ultrasonic treatment applied

The average yield strengths of the first, second, third, fourth, and fifth column samples not subjected to the ultrasonic treatment were 78.59 MPa, 79.95 MPa, 83.58 MPa, 91.75 MPa, and 101.90 MPa, respectively. The average yield strengths of the first, second, third, fourth, and fifth column samples subjected to the ultrasonic treatment were 85.02 MPa, 86.38 MPa, 90.21 MPa, 96.94 MPa, and 105.19 MPa, respectively. Compared with the samples not subjected to the ultrasonic treatment, the average yield strength of the samples subjected to the ultrasonic treatment increased by 8.18%, 8.04%, 7.93%, 5.66%, and 3.23% in columns 1, 2, 3, 4, and 5, respectively. The average yield strength improvement rate of the first column samples subjected to the ultrasonic treatment was the largest compared to the samples not subjected to the ultrasonic treatment.

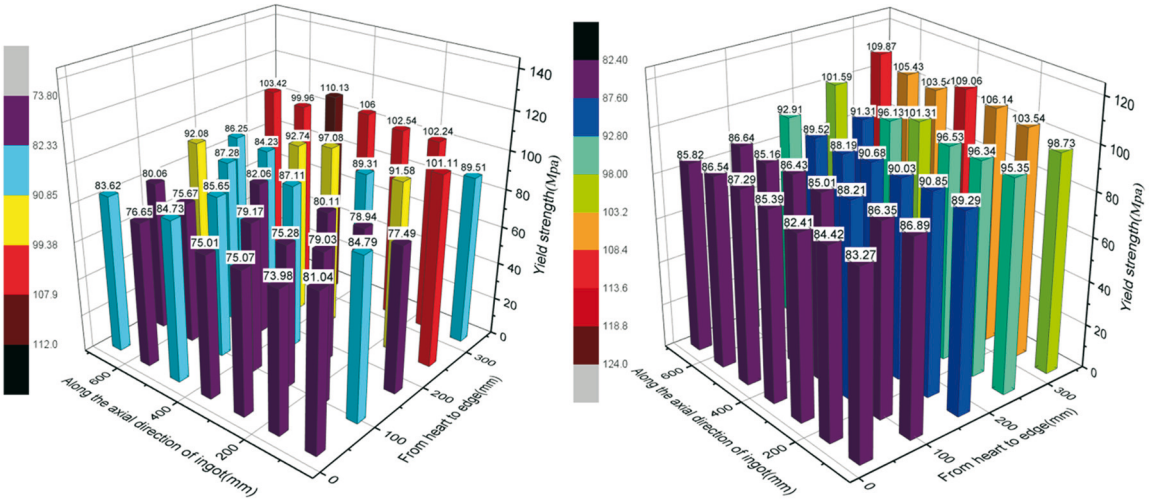

Fig. 5 Yield strength distribution of 1/2 longitudinal section of ingot:
(a) ultrasonic treatment not applied, (b) ultrasonic treatment applied

The average elongation of the first, second, third, fourth, and fifth column samples not subjected to the ultrasonic treatment was 3.77%, 4.23%, 5.06%, 6.65%, and 7.83%, respectively. The average elongation of the first, second, third, fourth, and fifth column samples subjected to the ultrasonic treatment was 5.17%, 5.75%, 6.67%, 8.36%, and 9.57%, respectively. Compared with the samples not subjected to the ultrasonic treatment, the average elongation of the samples subjected to the ultrasonic treatment increased by 37.15%, 35.93%, 31.82%, 25.71% and 22.22% in columns 1, 2, 3, 4, and 5, respectively. The average elongation improvement rate of the first column samples subjected to the ultrasonic treatment was the largest compared to the samples not subjected to the ultrasonic treatment.

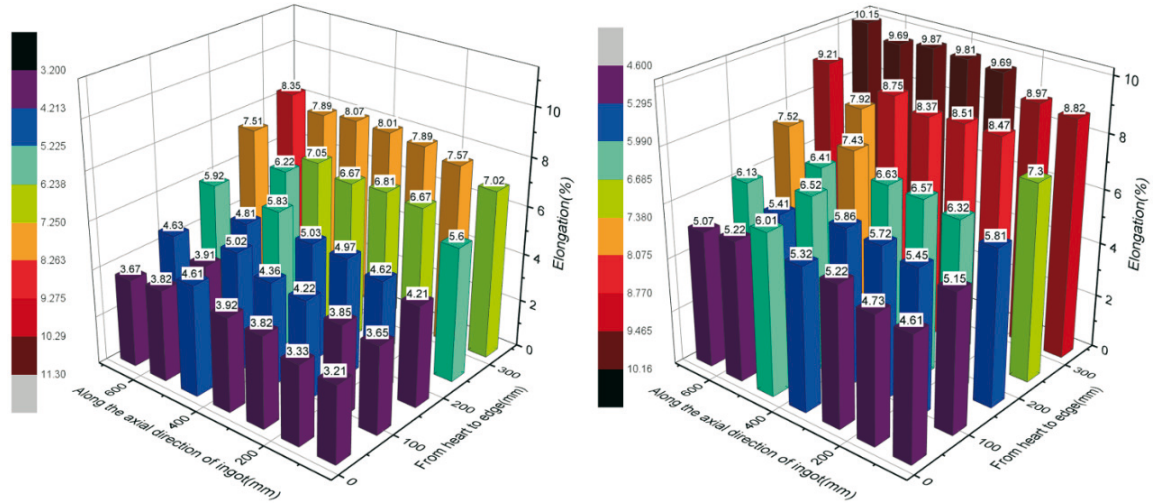

Fig. 6 Elongation distribution of 1/2 longitudinal section of ingot:
(a) ultrasonic treatment not applied, (b) ultrasonic treatment applied

The average tensile strength, average yield strength, and average elongation of the ingot not subjected to the ultrasonic treatment on the 1/2 longitudinal section were 169.50 MPa, 87.17 MPa, and 5.32%, respectively. The average tensile strength, average yield strength, and average elongation of the ingot subjected to the ultrasonic treatment on the 1/2 longitudinal section were 178.38 MPa, 92.75 MPa, and 7.10%, respectively. Compared with the ingot not subjected to the ultrasonic treatment, the average tensile strength, average yield strength and average elongation of the ingot subjected to the ultrasonic treatment increased by 5.24%, 6.40% and 33.46%, respectively.

On the longitudinal section, the average tensile strength, average yield strength, and average elongation of the ingot treated with ultrasound were improved as well as the overall performance of the ingot.

3.3 Analysis of fracture morphology

There were many tensile samples cut on the longitudinal section. By conducting a fracture morphology analysis of the samples from the centre to the edge, it was found that the patterns were somewhat similar. Therefore, only a portion of the images were selected, as shown in Fig. 7. Fig. 7(a), Fig. 7(b), Fig. 7(c) represent the fracture morphology at distances of 30 mm, 170 mm, and 310 mm from the centre of the ingot not subjected to the ultrasonic treatment, respectively. Fig. 7(d), Fig. 7(e), Fig. 7(f) represent the fracture morphology at distances of 30 mm, 170 mm, and 310 mm from the centre of the ingot subjected to the ultrasonic treatment, respectively. The cleavage surface and rough tearing edges represent typical brittle fracture characteristics. From Fig. 7(a), Fig. 7(b), Fig. 7(c) it can be seen that the ingot that was not subjected to the ultrasonic treatment has obvious tearing edges and large cleavage surfaces. The closer to the centre, the more obvious the tearing edges and cleavage surfaces. For the ingot treated with ultrasound, the analysis of the fracture morphology of the core sample revealed a significant reduction in the larger cleavage planes, but the tearing edges remained prominent. By comparing the fracture morphology of the samples at different positions, it was found that the ingot treated with ultrasound had reduced the larger cleavage planes and longer tearing edges.

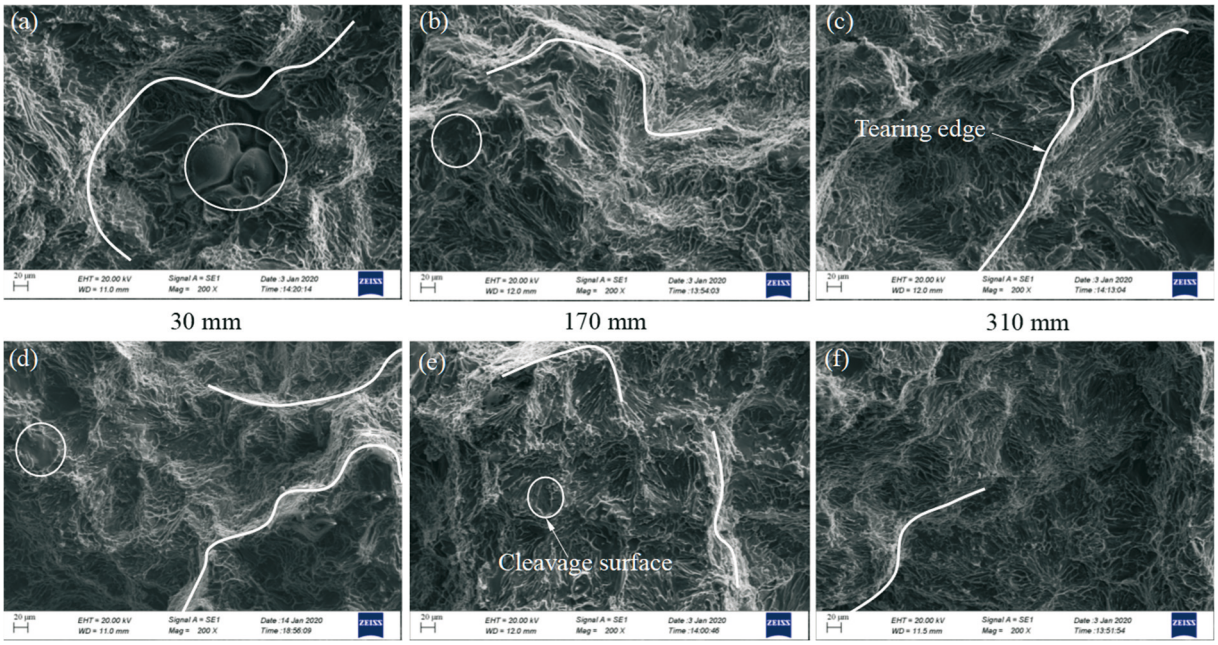

Fig. 7 (a), (b), (c) Fracture morphology at distances of 30 mm, 170 mm, and 310 mm from the centre of the ingot not subjected to ultrasonic treatment, respectively; (d), (e), (f) Fracture morphology at distances of 30 mm, 170 mm, and 310 mm from the centre of the ingot subjected to ultrasonic treatment, respectively

3.4 Analysis of eutectic structure

The surfaces of the samples were ground to achieve the desired surface roughness in order to observe their microstructure under an electron microscope. Fig. 8 shows the eutectic structure diagram, Fig. 8(a), Fig. 8(b) and Fig. 8(c) show the eutectic structure diagram of the sample taken at 30 mm, 170 mm and 310 mm away from the centre not subjected to the ultrasonic treatment, respectively. Fig. 8(d), Fig. 8(e) and Fig. 8(f) show the eutectic structure diagram of the sample taken at 30 mm, 170 mm and 310 mm away from the centre subjected to the ultrasonic treatment, respectively.

It can be seen from the SEM diagram presented in Fig. 8 that the bright colour region is the eutectic structure. The eutectic structure of ingots subjected or not subjected to the ultrasonic treatment has different degrees of enrichment at 30 mm, 170 mm and 310 mm away from the centre. The closer to the centre, the more obvious the enrichment of the eutectic structure. Compared with the ingot not subjected to the ultrasonic treatment, the eutectic structure aggregation of the ingot subjected to the ultrasonic treatment is restrained to a certain extent and the distribution is more balanced. On the ingot not subjected to the ultrasonic treatment, the shadow caused by the falling off of the eutectic structure appears at a distance of 30 mm from the centre.

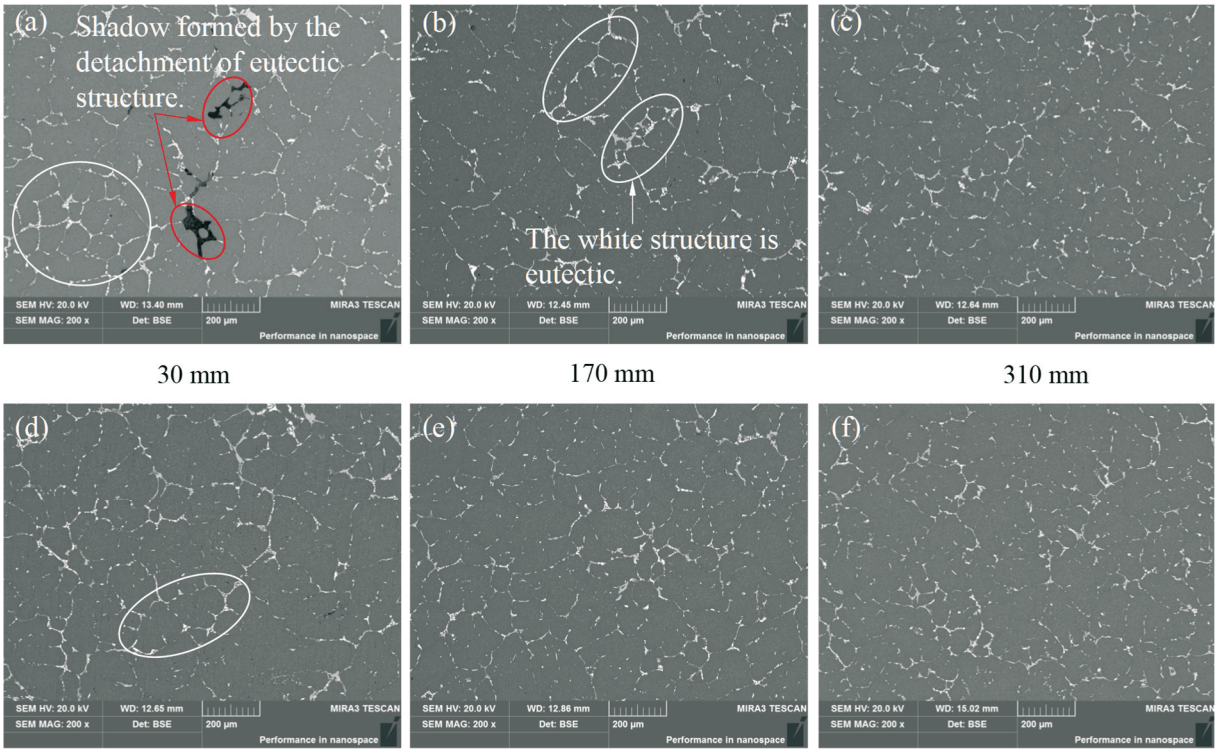

Fig. 8 (a), (b), (c) Eutectic structure at distances of 30 mm, 170 mm, and 310 mm from the centre of the ingot not subjected to ultrasonic treatment, respectively; (d), (e), (f) Eutectic structure at distances of 30 mm, 170 mm, and 310 mm from the centre of the ingot subjected to ultrasonic treatment, respectively

No obvious detachment of the eutectic structure was found in the samples treated with ultrasound. Therefore, after the ultrasonic treatment, the flow of the eutectic structure precipitated from the solid phase was promoted, the natural accumulation and brutal growth of the eutectic structure at the grain boundary was avoided, and the uniformity and compactness of the eutectic structure were promoted. As a result, the mechanical properties of the core tensile sample were improved and the overall comprehensive performance of the ingot was improved.

4. Conclusion

Composition determination, fracture analysis and eutectic structure analysis were conducted on the longitudinal section of the ingot. It was found that the ingots treated with ultrasound suppress macroscopic segregation, had fewer defects, and had a more uniform distribution of the eutectic structure. The specific conclusions were as follows:

(1) The segregation rates of Cu and Si elements on the 1/2 longitudinal section of the ingot not subjected to the ultrasonic treatment were 29.98% and 27.96%, respectively. The segregation rates of Cu and Si elements on the 1/2 longitudinal section of the ingot subjected to the ultrasonic treatment were 28.15% and 21.51%, respectively.

(2) The average tensile strength of the first column of samples not subjected to the ultrasonic treatment was 157.93 MPa, while the average tensile strength of the first column samples subjected to the ultrasound treatment was 167.81 MPa, which was 9.88 MPa higher than that not subjected to the ultrasonic treatment. The average tensile strength improvement rate of the first column samples subjected to ultrasound compared to the first column samples not treated with ultrasound was 6.25%. The average tensile strength of the second, third, fourth, and fifth column samples subjected to the ultrasonic treatment increased by 6.91%, 6.41%, 3.90%, and 3.25% compared to the samples not subjected to the ultrasonic treatment.

(3) The average yield strengths of the first, second, third, fourth, and fifth column samples not subjected to the ultrasonic treatment were 78.59 MPa, 79.95 MPa, 83.58 MPa, 91.75 MPa and 101.9 MPa, respectively. The average yield strengths of the first, second, third, fourth, and fifth column samples subjected to the ultrasonic treatment were 85.02 MPa, 86.38 MPa, 90.21 MPa, 96.94 MPa and 105.19 MPa, respectively. Compared with the samples not subjected to the ultrasonic treatment, the average yield strength of the samples subjected to the ultrasonic treatment increased by 8.18%, 8.04%, 7.93%, 5.66%, and 3.23% in columns 1, 2, 3, 4, and 5, respectively.

(4) The average elongation of the first, second, third, fourth, and fifth column samples not subjected to the ultrasonic treatment were 3.77%, 4.23%, 5.06%, 6.65% and 7.83%, respectively. The average elongation of the first, second, third, fourth, and fifth column samples subjected to the ultrasonic treatment were 5.17%, 5.75%, 6.67%, 8.36% and 9.57%, respectively. Compared with the samples not subjected to the ultrasonic treatment, the average elongation of the samples subjected to the ultrasonic treatment increased by 37.15%, 35.93%, 31.82%, 25.71% and 22.22% in columns 1, 2, 3, 4, and 5, respectively.

By conducting the mechanical performance testing, fracture morphology analysis, and eutectic structure analysis, the comprehensive properties of the ingot were improved after the ultrasonic treatment. The sound flow effect and cavitation effect generated by ultrasound in the aluminium melt made the distribution of solute elements more uniform, and the eutectic structure defects in the centre of the ingot were reduced. As a result, the overall comprehensive performance of the ingot was improved, which was verified by the mechanical performance testing of the samples.

Acknowledgments

This study was supported by the excellent youth project of the Department of Education of Hunan Province (19B389), the general programme of Hunan University of Arts and Science (SZZX2159), the Project of State Key Laboratory of High Performance Complex Manufacturing, Central South University (ZZYJKT2021-01), the Hunan Provincial Specialty Disciplines of Higher Education Institutions (XJT[2018]469), the Science and Technology Innovative Research Team in Higher Educational Institutions of Hunan Province (XJT[2019]379), and the Hunan University of Arts and Sciences Research Launch Project (23BSQD20).

REFERENCES

[1] Zhu C.; Zhao Z. H.; Zhu Q. F.; Wang G. S.; Zuo Y. B.; Qin G. W. Structures and macrosegregation of a 2024 aluminium alloy fabricated by direct chill casting with double cooling field, *China Foundry* **2022**,19(1), 1–8. https://doi.org/10.1007/s41230-022-1030-5

[2] Lin H.; Zhu K.; Liu Q.; Chen L.; Wang Z.; Li, X. Microstructural Characterization of the As-Cast and Homogenized Al-Cu-Mg-Ag Alloy, *Materials* **2023**, 16(1), 433. https://doi.org/10.3390/ma16010433

[3] Eskin, G.I. Broad prospects for commercial application of the ultrasonic (cavitation) melt treatment of light alloys, *Ultrasonics Sonochemistry* **2001**,8(3),319–325. https://doi.org/10.1016/s1350-4177(00)00074-2

[4] Eskin, D. G. Ultrasonic processing of molten and solidifying aluminium alloys: overview and outlook, *Materials Science and Technology* **2017**, 33(6): 636-645. https://doi.org/10.1080/02670836.2016.1162415

[5] Li R.; Liu Z.; Dong F.; Li X.; Chen P. Grain refinement of a large-scale Al alloy casting by introducing the multiple ultrasonic generators during solidification, *Metallurgical and Materials Transactions A* **2016**, 47: 3790-3796. https://doi.org/10.1007/s11661-016-3576-6

[6] Li R.; Liu Z.; Chen P.; Zhong Z.;Li X. Investigation on the Manufacture of a Large-Scale aluminium Alloy Ingot Microstructure and Macrosegregation, *Advanced Engineering Materials* **2017**, 19(2),1600375. https://doi.org/10.1002/adem.201600375

[7] Fezi K.; Plotkowski A.; Krane, M. J. M. Macrosegregation modeling during direct-chill casting of aluminium alloy 7050, *Numerical Heat Transfer, Part A: Applications* **2016**,70(9),939–963. https://doi.org/10.1080/10407782.2016.1214508

[8] Zeng T.; Zhou Y. J. Effects of ultrasonic introduced by L-shaped ceramic sonotrodes on microstructure and macro-segregation of 15t AA2219 aluminium alloy ingot, *Materials* **2019,** 12(19), 3162. https://doi.org/10.3390/ma12193162

[9] Peng H.; Li R.; Li X.; Ding S.; Chang M.; Liao L.; Zhang Y.; Chen P. Effect of multi-source ultrasonic on segregation of Cu elements in large Al-Cu alloy cast ingot, *Materials* **2019**, 12(17),2828. https://doi.org/10.3390/ma12172828

[10] Li A.; Jiang R.; Liu Z.; Li R.; Zhang Y. Effect of Multi-Source Ultrasonic on the Microstructure and Mechanical Properties of a Large Scale 2219 Al Alloy Ingot During Casting, *Frontiers in Materials* **2022**, 9, 796730. https://doi.org/10.3389/fmats.2022.796730

[11] Wang K.; Li R.; Jiang R.; ZHANG L.; LI X. Effect of Different-Source Ultrasonic Treatment on Intergranular Phase and Mechanical Properties of Large-Scale AlCu Ingots, *JOM* **2019**,71,4414–4423. https://doi.org/10.1007/s11837-019-03781-5

[12] Zhang L.; Li X.; Liu Z.; Li R.; Jiang R.; Guan S.; Liu B. Scalable ultrasonic casting of large-scale 2219AA Al alloys: Experiment and simulation, *Materials Today Communications* **2021**,27,102329. https://doi.org/10.1016/j.mtcomm.2021.102329

[13] Shi C.; Wu Y.; Mao D.; Fan G. Effect of Ultrasonic Bending Vibration Introduced by the L-shaped Ultrasonic Rod on Solidification Structure and Segregation of Large 2A14 Ingots, *Materials* **2020**,13(3), 807. https://doi.org/10.3390/ma13030807

[14] Meng Y.; Zhang H.; Li X.; Zhou X.; Mo VH.;Wang L.; Fan J. Tensile Fracture Behavior of 2A14 aluminium Alloy Produced by Extrusion Process, *Metals* **2022**,12(2),184. https://doi.org/10.3390/met12020184

[15] Liu Z.; Li R.; Jiang R.; Zhang L.; Li X. Scalable Ultrasound-Assisted Casting of Ultra-large 2219 Al Alloy Ingots, *Metallurgical and Materials Transactions A* **2019**,50(3),1146–1152. https://doi.org/10.1007/s11661-018-5097-y

[16] Chen P.; Zhang Y.; Li R. Effect of multi-source ultrasonic on segregation of Cu elements in large Al–Cu alloy cast ingot, *Materials*,**2019**, 12(17), 2828. https://doi.org/10.3390/ma12172828

Submitted: 11.12.2023

Accepted: 24.4.2024

Assist.Prof. Sichao Su*
Assoc. Prof. Yi Zhou
College of Mechanical Engineering, Hunan University of Arts and Sciences, Changde, China
Assist.Prof. Ruiqing Li
National Key Laboratory of High Performance Complex Manufacturing, School of Mechanical and Electrical Engineering & Light Alloy Research Institute, Central South University, Changsha, China
*Corresponding author:
susichao2022@163.com